JMEPEG (2012) 21:366–372
DOI: 10.1007/s11665-011-9908-1

1059-9495/$19.00

Effect of Aging on Superelastic Behaviors of a Metastable β Ti-Mo-based alloy

Jie Song, Xiaoning Zhang, Xiaogang Sun, Hong Jiang, Zhiguo Fan, Chaoying Xie, and M.H. Wu

(Submitted April 14, 2010; in revised form November 17, 2010)

Effect of aging on the tensile and superelasticity (SE) behaviors of Ti-9.8Mo-3.9Nb-2V-3.1Al (wt.%) alloy have been investigated. It is found that the ultimate tensile strength (UTS) and yield strength of aged alloy change with the aging temperature following a nonlinear relationship due to ω-phase and α-phase precipitates. The SE, especially elastic recovery behavior, is closely related with the morphology of α-phase precipitates, as well as ω-phase formed during aging. At a maximum tensile strain of 4%, the specimen aged at 673 K with ω + α-phase precipitates shows a superelastic recovery strain of 3.2%. Lots of α-phase precipitates, distributing homogeneously in specimen aged at 773 K, result in the lost of SE. A maximum recovery strain of 3.3% is obtained for specimens aged at 873 or 973 K for 30 min, with coarse short bar-like α-phase precipitates.

Keywords aging, precipitation, superelasticity, Ti-Mo-based alloy

1. Introduction

Recently, Ni-free β-type titanium alloys with shape memory effect (SME) and superelasticity (SE) have attracted attention as promising functional materials for medical applications (Ref 1). The Ti-*x*Mo-4Nb-2V-3Al (TMNVA) alloys are newly developed metastable β-Ti alloys for biomedical application with Mo-contents (*x*) in the range of 7.5-11.5 wt.% (Ref 2, 3), exhibiting SE of about 3% recovery strain after solution treatment at 1143 K. Zhang (Ref 4) studied the origin of SE of Ti-*x*Mo-4Nb-2V-3Al alloy and attributes the SE to a new reversible martensitic phase α‴. The microstructures, phase transformation, and mechanical properties of the Ti-Mo-based alloys have been investigated (Ref 5, 6). It is noticed that the SE of Ti-9.59Mo-3.98Nb-1.99V-3.13Al alloy has been improved after solution treated (ST) and flash annealing at temperature between 623 and 823 K for 10 s (Ref 7). Thermomechanical treatment is an effective way to improve the SME and SE (Ref 8). However, the microstructure evolution and precipitation during aging processes are still not well understood for Ti-*x*Mo-4Nb-2V-3Al alloys. In order to apply the thermomechanical treatment, e.g., severe plastic deformation (SPD) and aging to enhance the SME and SE of TMNVA alloy, a fully understanding of the precipitates during aging and the effect of aging on SME and SE is necessary. In this study, the effect of aging on the tensile and superelastic behaviors of Ti-9.8Mo-3.9Nb-2V-3Al alloy has been investigated systematically.

Jie Song, Xiaoning Zhang, Xiaogang Sun, Hong Jiang, Zhiguo Fan, and **Chaoying Xie**, State Key Lab. of Metal Matrix Composites, School of Materials Science and Engineering, Shanghai Jiao Tong University, Shanghai 200240, China; and **M.H. Wu**, Advanced Materials Technology, Edwards Life Sciences LLC, Irvine, CA. Contact e-mails: jies@sjtu.edu.cn and cyxie@sjtu.edu.cn.

2. Experimental Procedures

A Ti-9.8Mo-3.9Nb-2V-3.1Al wt.% (TMNVA) metastable β titanium alloy was received as hot rolled bars of 12 mm in diameter from Memry Corporation, USA. The as-received bars were ST at 1143 K for 1 h followed by quenching. Superelastic behavior of TMNVA alloy was analyzed by tensile test at room temperature. Specimens for tensile tests were cut from the ST bars and aged at a series of temperatures from 373 to 973 K for 30 min followed by quenching into water. The dimension of tensile specimens is shown in Fig. 1. Tensile tests were carried out under a strain rate of 1.0×10^{-4}/s. Strain were measured using a clip-on extensometer with a gauge length of 25 mm. Specimens for microstructure observation were mounted, polished, and then etched in a solution of water, nitric acid, and hydrofluoric acid with a volume fraction of 80:15:5. Phase constitution of polished solid specimen was identified by x-ray diffraction (XRD) with Cu $K\alpha_1$ radiation, obtained from a tube operated at 200 mA, 40 kV and the scan speed was 10°/s. For TEM observation, thin foil specimens were obtained by mechanical grinding to 80 μm thickness and twin jet eletropolishing (5% perchloric acid, 35% butyl alcohol, and 60% methyl alcohol; 30 V; 243 K). The chemical composition of TMNVA alloy specimens was assessed by energy dispersive x-ray (EDX) analysis. The EDX experiments were conducted using scanning electron microscope (JSM-6460).

3. Results and Discussion

3.1 Microstructures

Figure 2 and 3 shows the optical micrographs and the corresponding XRD results of specimens ST and aged at a

series of temperature from 573 to 973 K. It is seen in Fig. 2(a) and 3(a) that solution-treated specimen is single β-phase. After aging at 573 K for 30 min, the microstructure is almost the same as that of ST specimen, as shown in Fig. 2(b). However, the XRD result of 573 K aged specimen is different from that of ST specimen and a small peak of ω-phase appears as seen in Fig. 3(b). The ω-phase usually precipitates during aging at moderate temperature (Ref 9, 10). The dimension of ω-phase is so small that it is invisible under optical microscope and the transmission electron microscope (TEM) is usually applied to identify it.

As the aging temperature increased to 673 K, very fine precipitates appear in grains, as seen in Fig. 2(c). XRD result shows that the $(10\bar{1}2)_\omega$ peak of ω-phase exists and a very small $(10\bar{1}0)_\alpha$ peak of α-phase appears, as shown in Fig. 3(c), which reveals that ω-phase and α-phase coexisting. Figure 4 shows the ω-phase observed under TEM in specimen aged at 673 K for 30 min. The size of ω-phase is only about 10 nm.

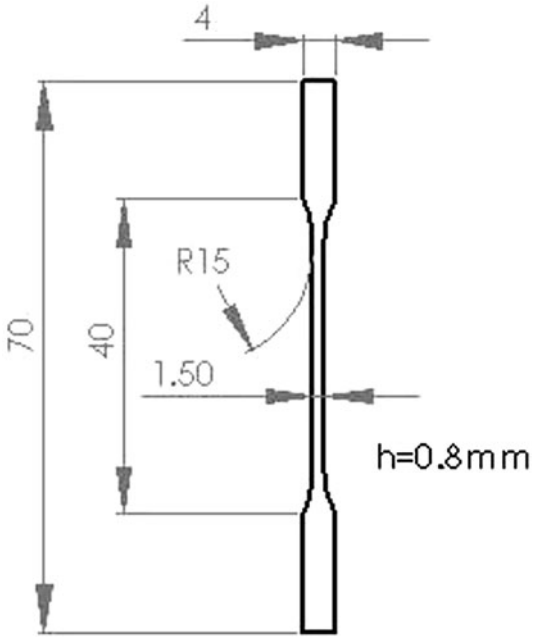

Fig. 1 The dimension of TMNVA alloy specimen for tensile test

It is noticed that there are bright zones along the grain boundary in Fig. 2(c), which are similar to the α-phase free areas (Ref 11). It is reported that the ω-phase precipitated as intermediate phase inside grains during aging at temperatures lower than 773 K and the ω-phase precipitates act as the nucleation site of α-phase preferentially. The α-phase nucleated and grew inside grains, so there formed the bright α-phase free zone along grain boundary (Ref 11, 12).

As the aging temperature increased to 773 K, lots of fine α-phase distribute in the grains homogeneously, as shown in Fig. 2(d), but ω-phase disappears as identified by XRD, shown in Fig. 3(d). It has been reported in Ref 11, 12 that when the aging temperature was higher than 773 K, the α-phase precipitated from β-phase directly, and the grain boundary was also the nucleation sites of α-phase for metastable β Ti-15Mo-2.7Nb-3Al-0.2Si alloy.

After aging at 873 K, coarse bar-like α-phase precipitates appear preferentially on the grain boundaries, which causes the grain boundaries coarse and dark, and a little α-phase precipitates inside grains, as shown in Fig. 2(e). There are very little α-phase precipitates inside the grains after aged at 973 K and small fish-bone like α-phase appears along the grain boundary. The fish-bone like α-phase is well developed after aging at 973 K for 1 h (Ref 13). It is clear seen that the grain boundaries are preferential nucleation sites for α-phase during aging at temperatures from 773 to 973 K.

Comparing $(10\bar{1}0)_\alpha$ peaks of α-phase in Fig. 3(c)-(f), it is clear that the amount of α-phase increases to a maximum value after aging at 773 K for 30 min.

3.2 Tensile Behavior

Figure 5(a) shows tensile stress-strain curves of the TMNVA alloy ST and aged at a serious of temperatures of 573-973 K for 30 min. The stress-strain curves can be classi-

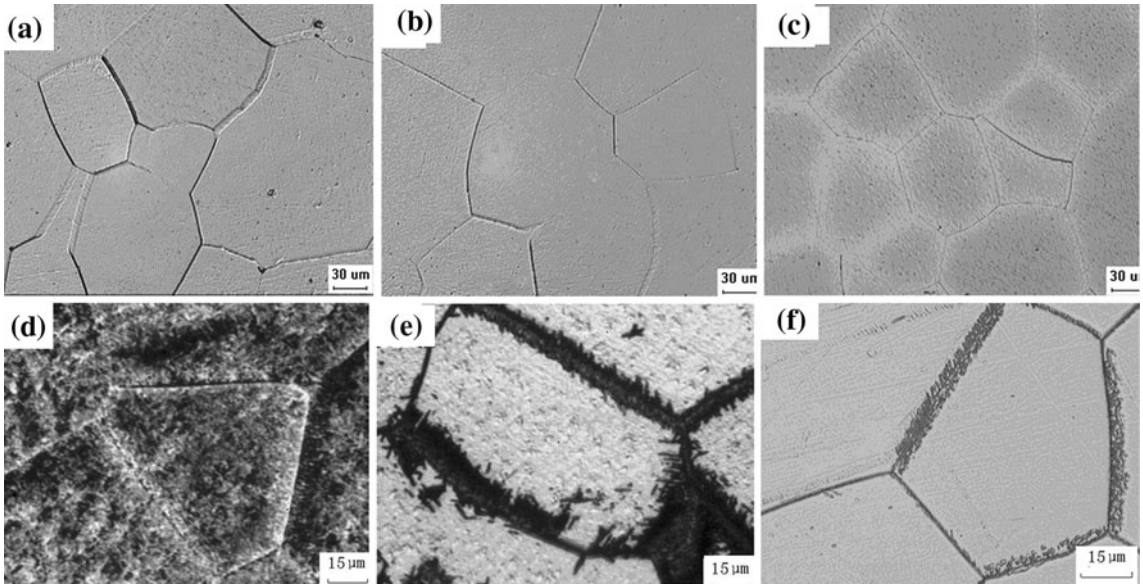

Fig. 2 Optical micrographs of TMNVA alloy specimens: (a) ST, and aged at (b) 573, (c) 673, (d)773, (e) 873, and (f) 973 K

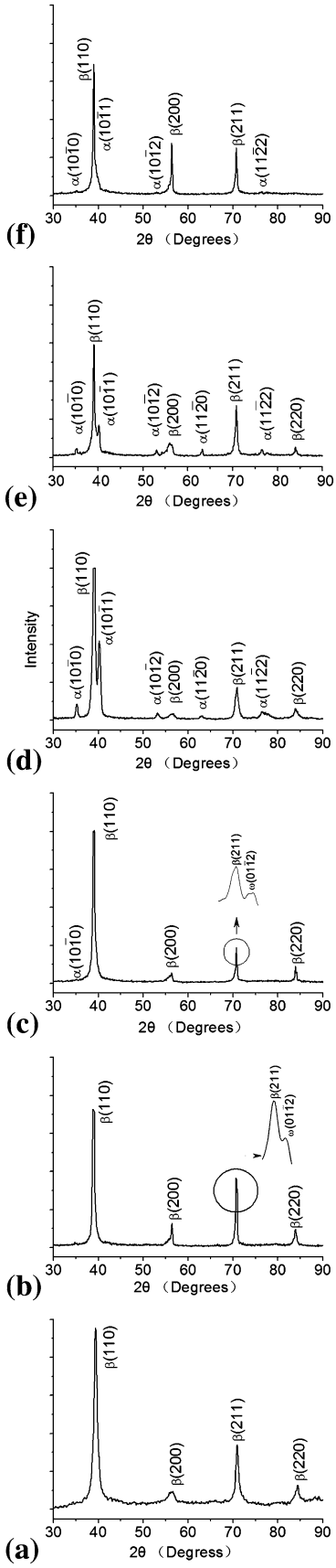

Fig. 3 XRD spectra for TMNVA alloy specimens: (a) ST and aged at (b) 573, (c) 673, (d) 773, (e) 873, and (f) 973 K

fied into three groups, as shown in Fig. 5(a) marked by I, II, and III, based on their yielding and strain hardening behaviors.

Group I, for the stress-strain curves showing work hardening after yielding. The specimen aged at 673 K belongs to group I, showing a similar deformation behavior to that of ST specimen, with obvious work hardening after yielding.

Group II, for the stress-strain curves showing little work hardening after yielding. Specimens aged at 573 and at 773 K belong to Group II.

Group III, for the stress-strain curves showing two yielding phenomena and a high work-hardening rate after the first yielding, but very small after the second yielding. Specimens aged at 873 and 973 K belong to group III. The ultimate tensile strength (UTS) and yield strength of aged specimens change with the aging temperature following a nonlinear relationship. The UTS decreases first with the aging temperature, to a minimum value (920 MPa) after aging at 573 K, then increases, to a maximum value (1240 MPa) after aging at 773 K, and decreases again with aging temperature, as shown in Fig. 5(b).

According to microstructure analysis of Fig. 2(a)-(d) and 3(a)-(d), it is reasonably suggested that lots of homogeneously distributed fine α-phase precipitates result in the maximum UTS of specimen aged at 773 K, as well as the lost of work hardening after yielding. The specimen aged at 573 K shows a similar tensile deformation behavior to that of 773 K aged specimen, but with much lower stress plateau (920 MPa), which reveals that the strengthening effect of fine ω-phase precipitates is less than that of fine α-phase precipitates.

It is noticed that the specimen aged at 573 K has a maximum elongation, larger than 9% showing no obvious embitterment, although there are ω-phase precipitates as identified in Fig. 3(b).

In order to investigate the deformation mechanism of the specimens belonging to above three groups, the microstructure observation and the XRD analysis are carried out after elongated at a strain of 4% and unloaded, as shown in Fig. 6. It is seen that all specimens exhibit needle-like microstructures. However, the XRD result shows that there is no any new diffraction peak emerged for the specimen aged at 573 K, which belongs to group II, comparing Fig. 6(b) with Fig. 3(b), which implies that there is no new phase formed during tensile deformation. The needle-like microstructure may be the deformation twin (Ref 14, 15).

In contrast, the XRD results for specimens, aged at 673 (belonging to group I) and 973 K (belonging to group III), after tensile deformation are different from those as aged, comparing Fig. 6 with Fig. 3. The $(111)_{\alpha''}$ peak is identified on spectrum of XRD as shown in Fig. 6(d, f), which reveals that the needle-like structure in these specimens is stress induced α″ phase (Ref 16). It is suggested that the deformation mechanism of the specimens belonging to group II is general plastic deformation, while the deformation mechanism, at least after the first yielding, of the specimens belonging to group I and group III is stress induced $\beta \rightarrow \alpha''$ transformation.

As seen in Fig. 5, the critical stress for inducing transformation $\beta \rightarrow \alpha''$ in specimen aged at 673 K, belonging to group I, is higher than that (i.e., the first yield stress) in specimens aged at 873-973 K, belonging to group III. It is suggested that the difference in stress-strain curves for specimens belonging to group I and group III maybe attribute to the driving force for the stress-induced transformation $\beta \rightarrow \alpha''$. The driving force of transformation $\beta \rightarrow \alpha''$ for group III, is

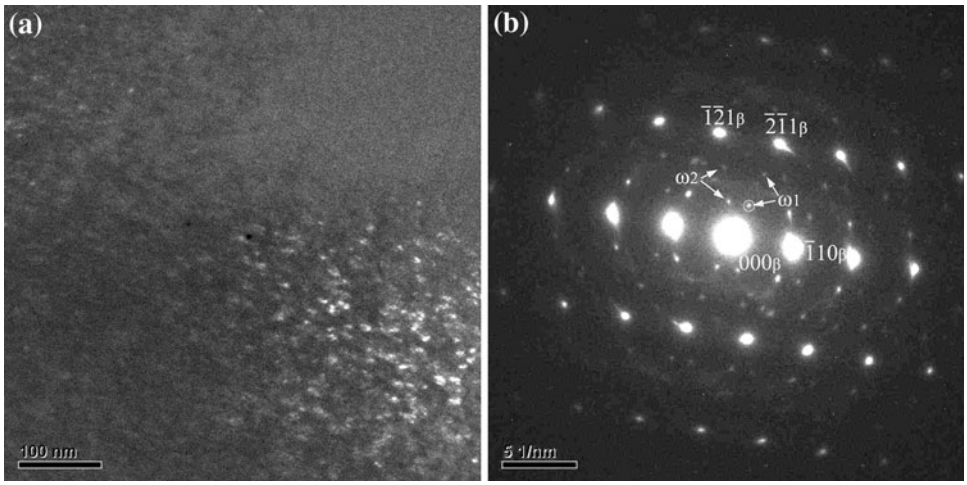

Fig. 4 TEM micrographs of TMNVA alloy specimen aged at 673 K for 30 min: (a) dark field image obtained with the diffraction spot marked with circle in (b); and (b) the corresponding select area diffraction pattern

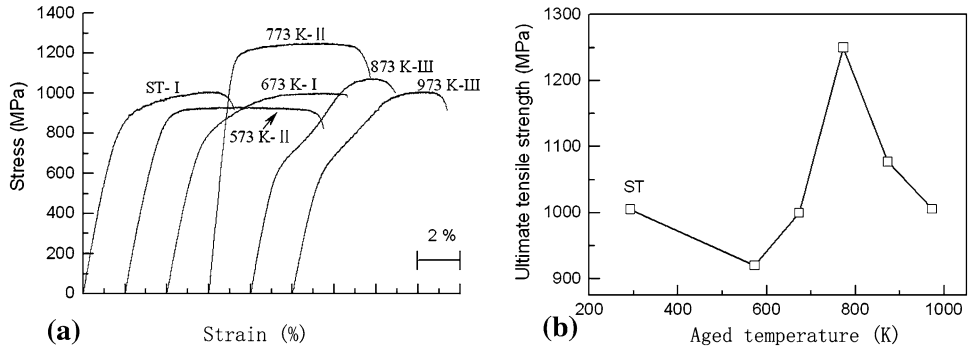

Fig. 5 The tensile curves (a) and UTS vs. aging temperature curve (b) of TMNVA alloy specimens solution treated (ST) and aged at 573-973 K for 30 min

lower than that of group I. The mechanism of effect of microstructures on the deformation behavior needs further investigation.

3.3 Superelastic Behavior

Usually, shape memory alloys exhibit SE, after the first yielding and unloading which is associated with the reversible stress-induced martensitic transformation or reorientation of martensitic variants (Ref 17, 18). The aged TMNVA specimens with three different shapes of stress-strain curves show different superelastic behaviors at a maximum strain of 4% as shown in Fig. 7, especially the unloading curves are different among the three groups.

It is seen in Fig. 7(a, b) that the specimens of ST and aged at 373 K (with stress-strain curves of Group I) show SE and have a recovery strain of 2.8-2.6%. However, during unloading, the unloading stress-strain curve is linear-like without stress plateau. For specimens aged at 473-523 K with stress-strain curves of group II in Fig. 5(a), no SE is observed, and only linear elastic strain of 1.2-1.4% recovered, as seen in Fig. 7(c, d). The SE is restored as the aging temperature increases from 623 to 723 K, as seen in Fig. 7(f-h), and the specimens show a similar superelastic behavior to that of ST and aged at 373 K specimens, with stress-strain curves of group I in Fig. 5(a). A recovery strain of 3.2% is obtained for specimens aged at 673 K, as shown in Fig. 7(g).

SE lost completely for specimen aged at 773-823 K with stress-strain curves of group II in Fig. 5(a), and only linear elastic strain of 1.6-1.7% recovered during unloading, as seen in Fig. 7(i, j). As aging temperature increases further, the SE is restored again and a maximum recovery strain of 3.3% is obtained for specimens aged at 873 and 973 K, as seen in Fig. 7(k, l), with stress-strain curves of group III in Fig. 5(a). It is noticed that a typical two-stage recovering behavior exhibits for those specimens, where there are first linear elastic recovery and then, nonlinear recovery with an obvious inflexion during unloading, which is well-known typical recovering behavior for shape memory alloys.

The decrease and lost of SE for specimens aged at 473-523 K may be attributed to the ω-phase precipitating, as detected by XRD in Fig. 3(b). The lost of SE for those specimens aged at 773-823 K is obviously attributed to the homogeneously distributed huge fine α-phase precipitates. However, some α-phase or α + ω-phase exist in specimens aged at 673 (Fig. 2c), 873, and 973 K (Fig. 2e, f), but good SE is obtained. It is reasonably suggested that a coarsening of α-phase or ω-phase precipitates is in favor of superelastic recovery, but fine homogeneously distributed α-phase precipitates or ω-phase precipitates constraint the superelastic recovery.

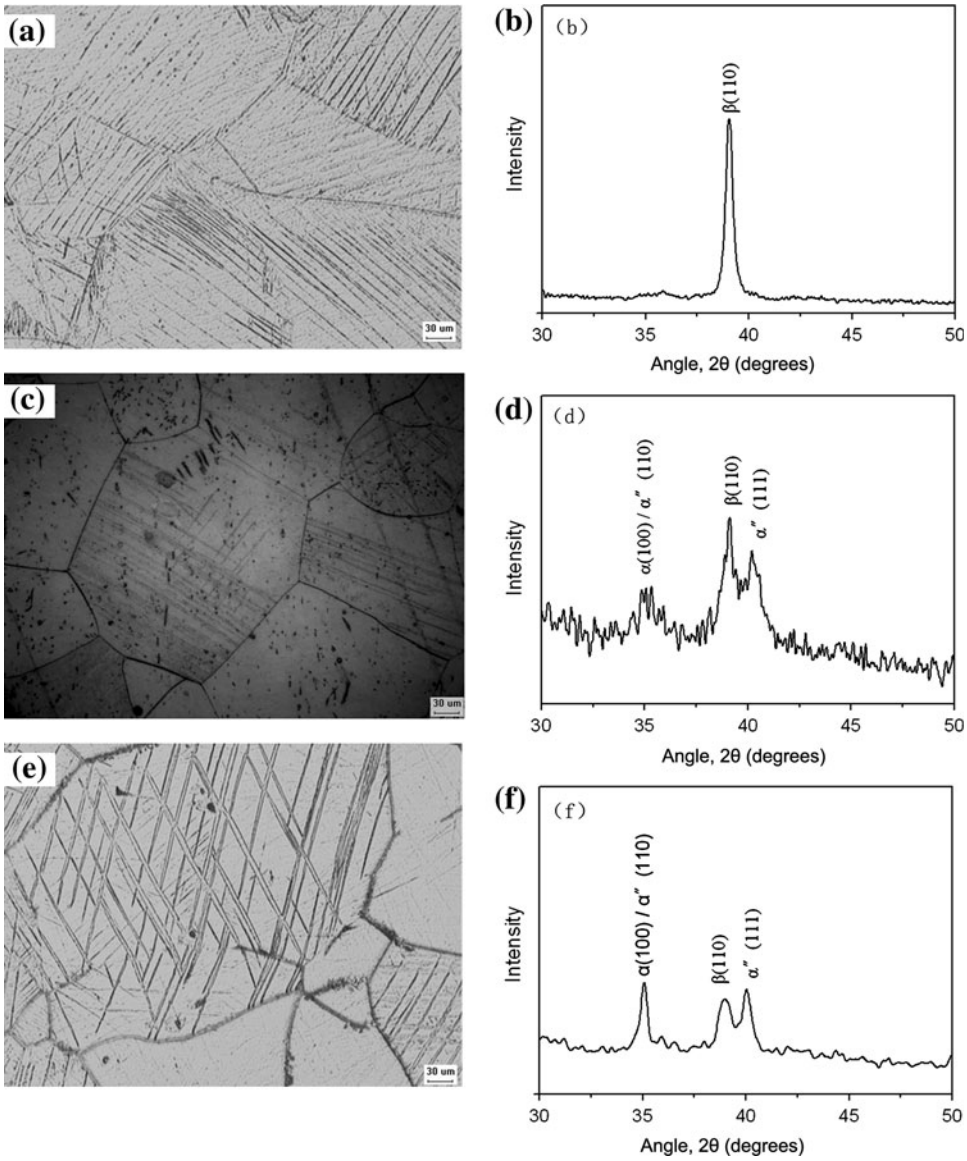

Fig. 6 Optical micrographs and XRD profiles of aged TMNVA alloy specimens after tensile test until failure; (a, b) aged at 573 K, (c, d) aged at 673 K, and (e, f) aged at 973 K

The effect of aging on the SE of TMNVA alloy maybe attribute to two reasons. One is the change of chemical composition in the matrix of aged specimens and the other is the micrograph of precipitated phase. For Ti-Mo or Ti-Nb-based β alloys, there are α-phase and ω-phase, both solute-lean, precipitation during aging and the matrix (β) becomes solute-rich after aging. As a result, the martensite start temperature (Ms) is lowered and the stress to induce martensite is increased by the aging (Ref 6, 19).

In order to evaluate the aging effect, the chemical composition change in the matrix of aged TMNVA alloy specimens were assessed by EDX method. The Mo content dependence of aged temperature for TMNVA alloy is shown in Fig. 8. It is seen that the Mo content increases with the aging temperature increases when aging temperature is <773 K. And as the aging temperature increases to 973 K, the Mo content decreases. The Mo content is higher than that of ST specimen, but $<11\%$ for specimens aged at 673, 873, and 973 K where some α-phase precipitates, as well as ω-phase precipitates. The martenstic transformation temperature decreases with the Mo content increases, which improve the SE, as seen in Fig. 7. A maximum Mo content is about 11.8% for specimen aged at 773 K, where lots of α-phase precipitates observed, as shown in Fig. 2, and this specimen does not exhibit superelasticity. It has been reported (Ref 18) that as the β-stable element (such as Mo, Nb, V, etc.) increase, the β-phase becomes more stable and the stress-induced martensitic transformation will not occur.

However, it is noticed that the specimen aged at 573 K does not exhibit SE, though it's Mo content is higher than that of ST specimen and $<11\%$, due to ω-phase precipitates. It seems that the lost of SE for specimen aged at 573 K may rise from other factor, such as the micrograph of precipitated phase and the plastic deformation ability of the precipitates,

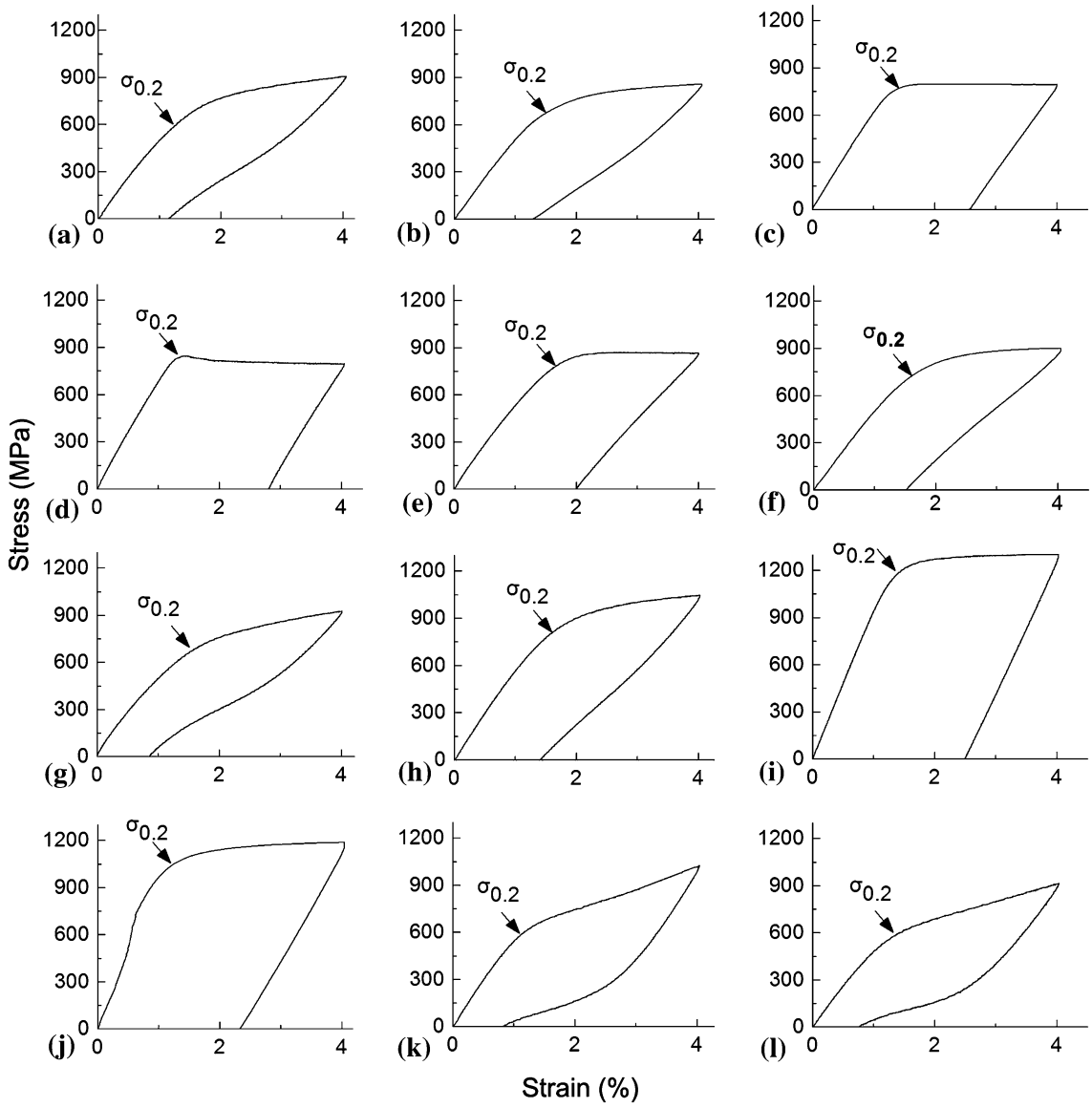

Fig. 7 Tensile curves of TMNVA alloy specimens solution treated (a) and aged at (b) 373, (c) 473, (d) 523, (e) 573, (f) 623, (g) 673, (h) 723, (i) 773, (j) 823, (k) 873, and (l) 973 K

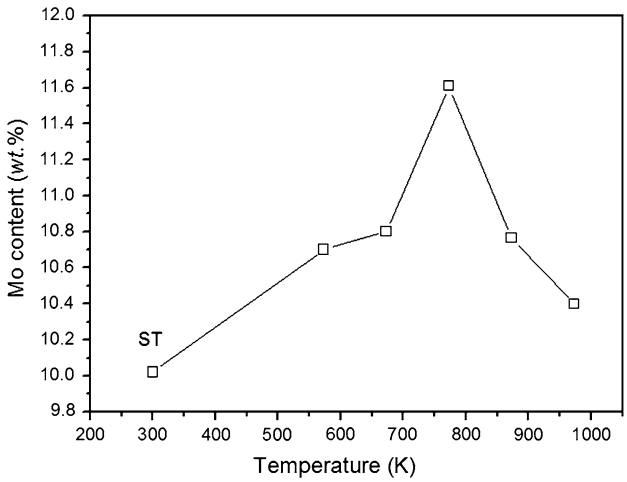

Fig. 8 Mo content dependence of aged temperature for TMNVA alloy specimens solution treated and aged at 573-973 K for 1.8 ks

besides the chemical change in the matrix. The mechanism for the effect of α-phase precipitates, as well as ω-phase precipitates, with different morphologies and Mo content on superelastic behavior is not clear completely and still under investigation by in situ TEM.

4. Conclusions

The effect of aging on tensile and superelastic behaviors of the metastable β Ti-Mo-based TMNVA alloy was investigated. The results are summarized as follows:

(1) The UTS of aged TMNVA alloy change with the aging temperature following a nonlinear relationship. Fine α-phase precipitates, distributing homogeneously, result in a maximum UTS and the lost of superelasticity. The superelastic behavior is closely related with the

morphology of α-phase precipitates, as well as ω-phase precipitates formed during aging.

(2) When aged at 673, 873, or 973 K for 30 min, TMNVA alloy shows good SE. At a maximum tensile strain of 4%, the specimen aged at 673 K with ω + α-phase precipitates shows superelastic recovery strain of 3.2%. Specimens aged at 473-523 K and 773-823 K for 30 min lost superelasticity completely. A maximum recovery strain of 3.3% is obtained for specimens aged at 873 and 973 K for 30 min, with coarse short bar-like α-phase precipitates along grain boundaries and a few inside grains.

Acknowledgments

We thank for the financial support from the National Science Fund of China (No. A50671067), and we thank for support from The Science and Technology Committee of Shanghai Municipal (09JC1407200).

References

1. N.T.C. Oliveira, G. Aleixo, R. Caram, and A.C. Guastaldi, Development of Ti-Mo Alloys for Biomedical Applications: Microstructure and Electrochemical Characterization, *Mater. Sci. Eng. A*, 2007, **452–453**(15), p 727–731
2. T. Zhou, M. Aindow, S.P. Alpay, M.J. Blackburn, and M.H. Wu, Pseudo-Elastic Deformation Behavior in a Ti/Mo-Based Alloy, *Scr. Mater.*, 2004, **50**(3), p 343–348
3. P.A. Russo, M.H. Wu, and J.G. Ferrero, Pseudoelastic Beta Ti-Mo-V-Nb-Al Alloys, *Proceedings, International Conference on Shape Memory and Superelastic Technologies (SMST-2003)*, Pacific Grove, CA, 2003
4. T. Zhou, L.C. Zhang, S.P. Alpay, M. Aindow, and M.H. Wu, Origin of Pseudoelastic Behavior in Ti-Mo-Based Alloys, *Appl. Phys. Lett.*, 2005, **87**, p 241909 (1-3)
5. E. Sukedai, D. Yoshimitsu, H. Matsumoto, and H. Hashimoto, Kiritani. β to ω Phase Transformation Due to Aging in a Ti-Mo Alloy Deformed in Impact Compression, *Mater. Sci. Eng. A*, 2003, **350**(1–2), p 133–138
6. W.F. Ho, C.P. Ju, and J.H. Chern Lin, Structure and Properties of Cast Binary Ti-Mo Alloys, *Biomaterials*, 1999, **20**(22), p 2115–2122
7. T. Zhou, M. Aindow, S.P. Alpy, M.J. Blackburn, and M.H.Wu, Phase Transformations and Mechanical Response in a Ti/Mo-Based Pseudo-Elastic Alloy, *Proceedings, International Conference on Shape Memory and Superelastic Technologies (SMST-2003)*, Pacific Grove, CA, 2003
8. H.Y. Kim, J.I. Kim, T. Inamura, H. Hosoda, and S. Miyazaki, Effect of Thermo-Mechanical Treatment on Mechanical Properties and Shape Memory Behavior of Ti-(26-28) at.% Nb Alloys, *Mater. Sci. Eng. A*, 2006, **438–440**(25), p 839–843
9. A.W. Bowen, Strength Enhancement in a Metastable β-Titanium Alloy: Ti-15Mo, *J. Mater. Sci.*, 1977, **12**(7), p 1355–1360
10. P. Ganesan, G.A. Sargent, and R.J. De Angelis, Relationship Between the Structure and Mechanical Properties in β III, Titanium Alloy, *J. Mater. Sci.*, 1980, **15**(6), p 1425–1435
11. P.L. Ferrandini, F.F. Cardoso, S.A. Souza, C.R. Afonso, and R. Caram, Aging Response of the Ti-35Nb-7Zr-5Ta and Ti-35Nb-7Ta Alloys, *J. Alloys Compd.*, 2007, **433**(1–2), p 207–210
12. S.G. Xu Bin and X. Peng Yiqun Tuo, Phase Transformation in Ti-15Mo-2.7Nb-3Al-0.2Si High Strength Titanium Alloy, *J. Mater. Eng.*, 1999, **3**, p 19–23 (in China)
13. C.X. Jie Song, α Phase Forming on Surface Layer and Precipitating Inside of a Ti-Mo Based Alloy Annealed in Air, *Adv. Mater. Res.*, 2007, **26–28**, p 1295–1298
14. S. Hanada and O. Izumi, Transmission Electron Microscopic Observations of Mechanical Twinning in Metastable Beta Titanium Alloys, *Metall. Trans. A*, 1986, **17**(8), p 1409–1420
15. S. Hanada and O. Izumi, Deformation of Metastable BetaTi-15Mo-5Zr Alloy Single Crystals, *Metall. Trans. A*, 1980, **11**(8), p 1447–1452
16. L.C. Zhang, T. Zhou, M. Aindow, S.P. Alpay, M.J. Blackburn, and M.H. Wu, Nucleation of Stress-Induced Martensites in a Ti/Mo-Based Alloy, *J. Mater. Sci.*, 2005, **40**(11), p 2833–2836
17. T. Grosdidier, C. Roubaud, M.-J. Philippe, and Y. Combres, The Deformation Mechanisms in the β-Metastable β-Ce Titanium Alloy, *Scr. Mater.*, 1997, **36**(1), p 21–28
18. T. Grosdidier and M.J. Philippe, Deformation Induced Martensite and Superelasticity in a β-Metastable Titanium Alloy, *Mater. Sci. Eng. A*, 2000, **291**(1–2), p 218–223
19. H.Y. Kim, H. Satoru, J.I. Kim, H. Hosoda, and S. Miyazaki, Mechanical Properties and Shape Memory Behavior of Ti-Nb Alloys, *Mater. Trans.*, 2004, **45**(7), p 2443–2448